

RESEARCH PAPER

TiO₂/ZnO/Bi₂O₃ Ternary Mixed Metal Oxide as an Efficient Visible Light Photocatalyst for Degradation of Methylene Blue

Abdul Amir H. Kadhum ¹, Huda Hadi Nameh ², Zaid H. Mahmoud ³, Sudad Jasim Mohammed ^{4*}, Mahdi M. Hanoon ⁵, Ahmed A. Alamiery ⁶, Adil Turki Al-musawi ⁴, Muslim Mhaibes, Raed ⁷

¹ College of Medicine, University of Al-Ameed, Karbala, Iraq

² College of Pharmacy, University of Hilla, Babylon, Iraq

³ Chemistry Department, College of Sciences, University of Diyala, Iraq

⁴ Market Research and Consumer Protection Center, University of Baghdad, Iraq

⁵ Protection and Metallurgy Engineering Department, University of Technology, Iraq

⁶ Al-Ayen Scientific Research Center, Al-Ayen Iraqi University, An Nasiriyah, Iraq

⁷ Department of Biochemistry, College of Medicine, Massan university, Missan, Iraq

ARTICLE INFO

Article History:

Received 17 April 2025

Accepted 25 June 2025

Published 01 July 2025

Keywords:

Methylene blue

Photocatalyst

Sol-gel method

Ternary mixed metal

nanoparticles

Visible light

ABSTRACT

This work reports sol-gel synthesis of ternary mixed metal oxide nanoparticles comprising TiO₂, ZnO, and Bi₂O₃. The structure and morphology of the nanoparticles were studied using XRD and FESEM. The Studying of optical properties of the nanoparticles showed the potential of the synthesized nanoparticles serving as an efficient photocatalyst for degradation of pollutant. It was found that the incorporation of Bi₂O₃ and ZnO has considerable impact on reducing of the TiO₂ band gap to 2.64 eV. The photocatalytic activity of the nanoparticles was investigated by visible light degradation of aqueous solution of methylene blue (MB). After 180 min illumination under visible light, the synthesized mixed metal oxide nanoparticles degraded the MB solution by 87%. Effect of different determinants, such as amount of photocatalyst, concentration of H₂O₂, and pH of MB solution, on the photocatalytic degradation of MB was studied.

How to cite this article

Kadhum A., Nameh H., Mahmoud Z. et al. TiO₂/ZnO/Bi₂O₃ Ternary Mixed Metal Oxide as an Efficient Visible Light Photocatalyst for Degradation of Methylene Blue. J Nanostruct, 2025; 15(3):1186-1194. DOI: 10.22052/JNS.2025.03.036

INTRODUCTION

Over the few decades, development of industrial and agricultural activities has resulted to vast environmental crisis in all over the world [1-3]. Oceans, lakes and rivers have been polluted by variety of toxic chemicals used in factories and farms. Surfactants, oils, organic chemicals, dyes, pesticides, insecticides, and fertilizers are the pollutants that are profusely discharged into water resources [1, 4]. These pollutants have

* Corresponding Author Email: sudad@mracpc.uobaghdad.edu.iq

accumulated in plants, fish and other aquatic beings that figured most of human diets in the some parts of the world. As a consequence, dangerous and chronic diseases have been developed in the human communities. Due to non-biodegradability of these compounds, the common treatment methods, such as biological, chemical and physical methods, do not provide satisfying results in removal of the pollutants from water [5, 6].



This work is licensed under the Creative Commons Attribution 4.0 International License.

To view a copy of this license, visit <http://creativecommons.org/licenses/by/4.0/>.

Fortunately, photocatalytic process has inspired scientists to eventually overcome this life threatening crisis [7]. The photocatalytic process utilizes a light-sensitive photocatalyst materials—a semiconductor—to produce highly activated radicals which are able to mineralize pollutants in aqueous media [8, 9]. The photocatalyst materials absorb the light beams with appropriate energy to excite the electrons from the valence band to the conduction band and leave behind the positively charged holes [10, 11].

Despite of the attractive performance of the photocatalytic process, there are some drawbacks that limit its use in the effective removal of the toxic pollutants [12, 13]. For instance, common photocatalyst materials such as TiO₂ (3.0-3.2 eV) and ZnO (3.2 eV) have a wide band gap which implies they can be activated by the shorter wavelength of the light spectrum; only UV light have the sufficient energy corresponded to such a wide band gap [14, 15]. Besides, fast recombination of the electrons and holes is the another limitation which are needed to improve before utilizing the photocatalyst process for treatment of the polluted water [16, 17].

Some strategies have been suggested to sensitize the photocatalyst materials for the visible light and reduce recombination rate of charge carriers (e⁻/h⁺) [18, 19]. In this regard, the photocatalyst materials comprising of different semiconductors have provided considerable efficiency for the degradation of organic pollutant in water media [20-24]. Different energy levels of the different photocatalysts ensure the electrons migration from one component to another [25, 26]. Moreover, the use of the lower band gap photocatalyst (such as WO₃ (2.8 eV), Bi₂O₃ (2.6 eV), etc.) can act as the visible light sensitizer and inject the electrons into the conduction band of another photocatalyst (TiO₂) [27-29]. For example, the enhanced photocatalytic activity for hydrogen evolution was reported for the binary nanocomposite comprising NiO/Bi₂O₃ [30]. Venkatwsh et. Al. synthesized Z-scheme ZnO/g-C₃N₄/V₂O₅ nanocomposite for the photocatalytic degradation of a mixed solution of dye and pharmaceutical compound under visible light irradiation [31]. Also, Naeinian et. al. studied the photocatalytic activity of CoFe₂O₄/Bi₂MoO₆ [32].

Herein, we have synthesized a ternary mixed metal oxide containing TiO₂, ZnO, and Bi₂O₃ using straightforward sol-gel reaction. The optical

properties of the nanoparticles was studied using DRS and PL analysis. The photocatalytic behavior of the prepared nanoparticles was evaluated using methylene blue (MB) aqueous solution under the visible light irradiation.

MATERIALS AND METHODS

Sol-gel synthesis of TiO₂/ZnO/Bi₂O₃ nanoparticles

One-pot synthesis of the ternary mixed metal oxide of TiO₂/ZnO/Bi₂O₃ nanoparticles (TZB) was accomplished using simple and facile sol-gel method, as follows: First, 0.5 mmol of citric acid as complexing agent was dissolved in 50 mL of absolute ethanol. Then, 1 mmol of tetrabutyl orthotitanate (TBOT) and certain amount of Zn(NO₃)₂·6H₂O (0.25, 0.5, and 0.75 mmol) were added slowly and stirred for 15 min. Bismuth precursor (Bi(NO₃)₃·5H₂O) (0.25, 0.5, and 0.75 mmol) was dissolved into 5 mL of deionized acidified by addition of certain amount of HNO₃, and then dropwise added into the above solution. The mixture was stirred for 1 hour and then kept in darkness for 12 hours to complete the reaction. After that, the solution was dried in an oven for 24 hours at 60 °C. The dried gel was pulverized in a mortar and then calcined at 700 °C for 5 hours. The parallel reaction method was followed to synthesized pure TiO₂ sample without addition of zinc and bismuth precursors.

Characterization

The phase structure of the synthesized nanoparticles was studied by the X-ray diffraction (XRD) patterns (Philips X'pert Pro MPD, Cu K α radiation λ = 1.54 Å). The composition and morphology of the synthesized nanoparticles were characterized using energy dispersive X-ray (EDX) and field emission scanning electron microscope (FESEM) by TESCAN Mira3. The optical properties of the TZB nanoparticles was studied using UV-Vis diffuse reflectance (DRS) spectroscopy using JASCO UV-Vis/NIR spectrophotometer. Also, the photoluminescence (PL) spectroscopy was used for studying the efficiency of the photo-generated charge carriers of the TZB nanoparticles by Perkin Elmer LS 55 spectrofluorometer.

Photocatalytic investigations

The photocatalytic activity of the synthesized TZB photocatalyst was evaluated for degradation of methylene blue (MB) under the visible light irradiation. A 100 W white color LED lamp was

used as the visible light source, and distance between the lamp and dye solution container was kept constant of 30 cm. Different amounts of the synthesized photocatalyst were dispersed into 50 mL of MB solution (50 ppm) in order to find optimum amount of the photocatalyst. In addition, the degradation reaction was carried out in different pH of MB solution, and the effect of oxidant agent (H₂O₂) was also investigated on the photocatalytic efficiency of the prepared photocatalyst.

Before illuminating by the visible light, the dispersion of TZB photocatalyst and MB solution was kept in darkness for 30 min under vigorous stirring to reach the adsorption/desorption equilibrium. After that, the photocatalytic reaction was initiated by turning on the LED lamp. The photocatalytic degradation of MB solution was studied in span of 180 min. Every 30 min, 5 mL of dye solution was collected and then centrifuged at 6000 rpm for 15 min to separate the photocatalyst particles. The level of degradation was evaluated using UV-Vis spectrophotometer at maximum absorption wavelength of MB ($\lambda_{\text{max}} = 668 \text{ nm}$).

RESULTS AND DISCUSSION

Structure, morphology, and optical properties

The XRD patterns for the pure TiO₂ and TiO₂/ZnO/Bi₂O₃ nanoparticles are provided in Fig. 1. The diffraction planes for the TZB nanoparticles are corresponded to the three components of the sample. The diffraction planes for the TiO₂ phase (marked with ⊗) are observed at 2 θ of 25.3°, 37.7°, 47.9°, 53.7°, 55.1°, 62.8°, 68.1°, 70.4°, and

74.9°. The Bragg positions corresponded to the ZnO phase (marked with ●) are centered at 2 θ of 31.9°, 34.7°, 36.2°, and 56.8. In addition, the Bi₂O₃ (marked with ♣) reflections are occurred at angles of 27.7°, 32.8°, and 53.7°. The peaks related to the ZnO and Bi₂O₃ phases are intensified with increasing the concentration of the ZnO and Bi₂O₃ in the sample. The XRD pattern for the pure TiO₂ reveals the formation of anatase phase (JCPDS file no. 04-0477).

Using the Scherrer equation [15], the average size of crystallite was calculated for the prepared samples. By considering the TiO₂ diffraction plane at 25.3°, the average crystallite size for the pure TiO₂, 0.25-TZB, 0.5-TZB, and 0.75-TZB are as 18.23 nm, 23.11 nm, 25.48 nm, 27.14 nm, and 29.01 nm, respectively. The increase in the crystallite size values is explained by the expansion of the unit cell of TiO₂ with increasing concentration of the ZnO and Bi₂O₃ phases into the TiO₂ matrix.

The morphology of the prepared TZB nanoparticles was studied using FESEM image, shown in Fig. 2. FESEM image (Fig. 2a) represents the semi-spherical nanoparticles in the size range of 50-200 nm. Moreover, EDX spectrum, shown in Fig. 2b, shows the composition of the TZB nanoparticles and confirms the presence of ingredients with relative amounts as follows: Ti (21.31 wt%), Zn (9.34 wt%), Bi (28.46 wt%), and O (40.89 wt%).

In order to validate the potential of TZB nanoparticles acting as the efficient photocatalyst, the optical behavior of the nanoparticles was studied using DRS and PL analysis. The Fig.

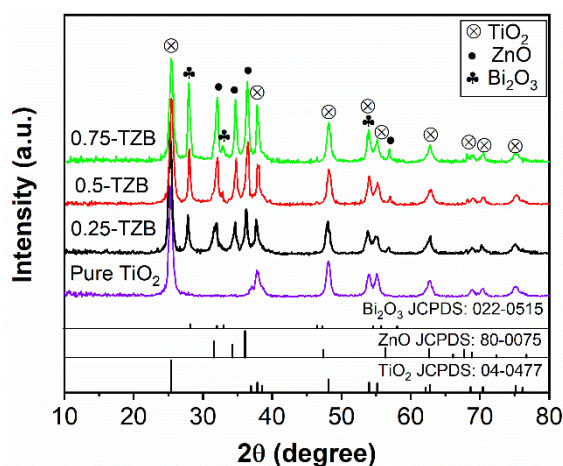


Fig. 1. XRD patterns for the synthesized nanoparticles.

3a shows the UV-Vis spectra for the different synthesized nanoparticles including: pure TiO_2 , 0.75-TBZ, 0.5TZB, and 0.25-TZB. As can be seen from the Fig. 3a, increasing the concentration of ZnO and Bi_2O_3 as visible light sensitizer leads to the enhancement of the absorption of light in the visible light region. However, further amount of the ZnO and Bi_2O_3 (0.75 mmol) has adverse effect on the visible light absorption ability of the TZB nanoparticles. The band gap values were calculated using plots of $(\alpha h\nu)^2$ vs. $h\nu$, which

confirm the 0.5-TZB nanoparticles (2.64 eV) have the lowest value of the band gap, shown in Fig. 3b. The calculated band gap for other samples are 2.85 eV, 2.92 eV, and 3.39 eV for the 0.25TZB, 0.75-TZB, and pure TiO_2 .

More consideration was taken into account to comprehend the optical properties of the synthesized TZB nanoparticles using PL analysis. Fig. 4 indicates that the 0.5-TZB nanoparticles have the lowest PL intensity compared to the other samples. This observation explains that

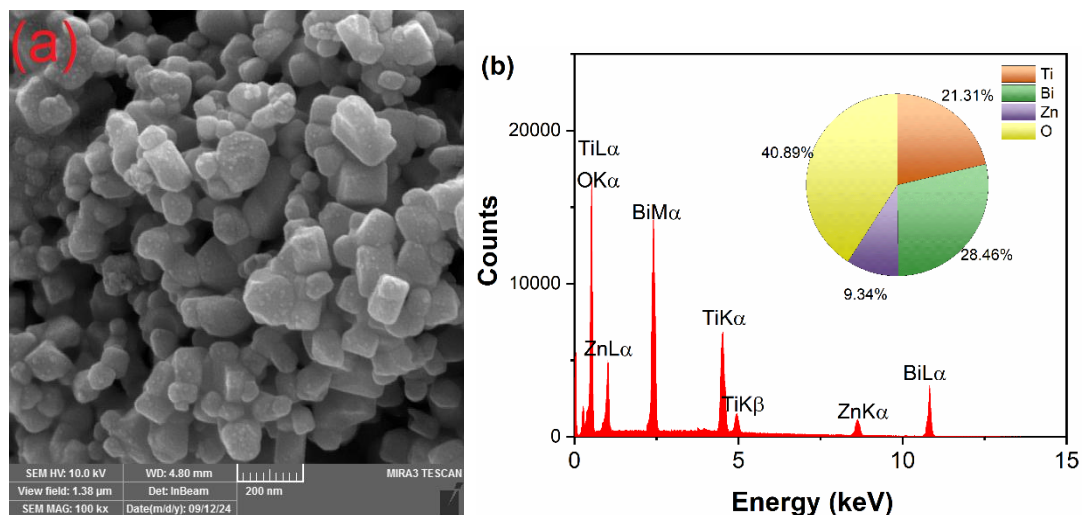


Fig. 2. FESEM image (a) and EDX spectrum (b) for the 0.5-TZB nanoparticles.

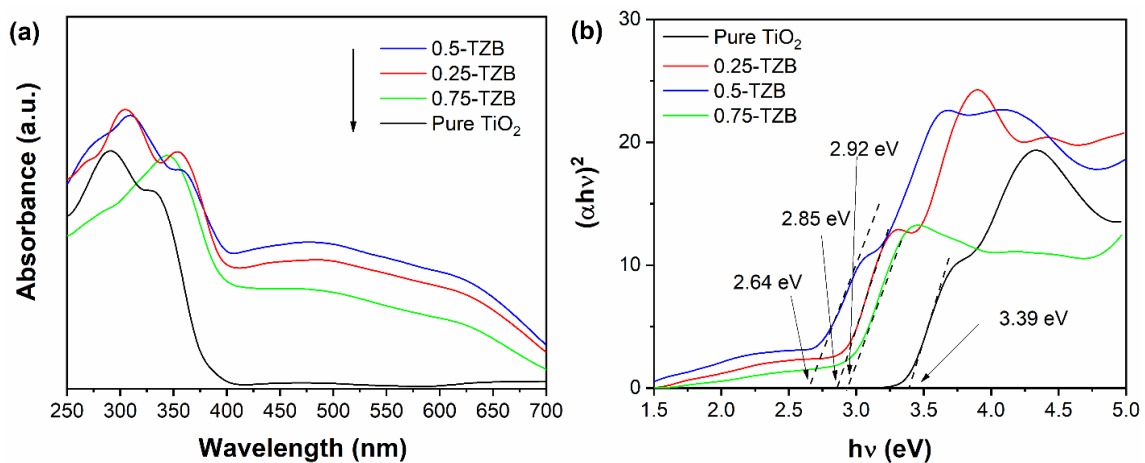


Fig. 3. DRS spectra (a) and plots of $(\alpha h\nu)^2$ vs. $h\nu$ (b) for the different synthesized nanoparticles.

the recombination of charge carriers takes place in the lower rate for the 0.5-TZB nanoparticle, which is the direct result of incorporation of Bi_2O_3 and ZnO phases into TiO_2 matrix. The transitions of the photo-generated electrons between the conduction bands of the well-mixed three semiconductors significantly reduce the recombination rate of the electrons and holes [5].

Photocatalytic properties

Fig. 5 shows the photocatalytic degradation

of MB solution over the different synthesized photocatalysts. Owing to the enhanced visible light absorption and separation of charge carriers, the 0.5-TZB nanoparticles possess higher photoactivity. Therefore, more than 87% of the MB solution was degraded using the 0.5-TZB photocatalyst. Other exploited photocatalyst including 0.25-TZB, 0.75-TZB, and pure TiO_2 provided the photocatalytic efficiency of 71%, 60%, and 32%, respectively. Also, Fig. 5 shows the self-degradation of MB solution under 180 min

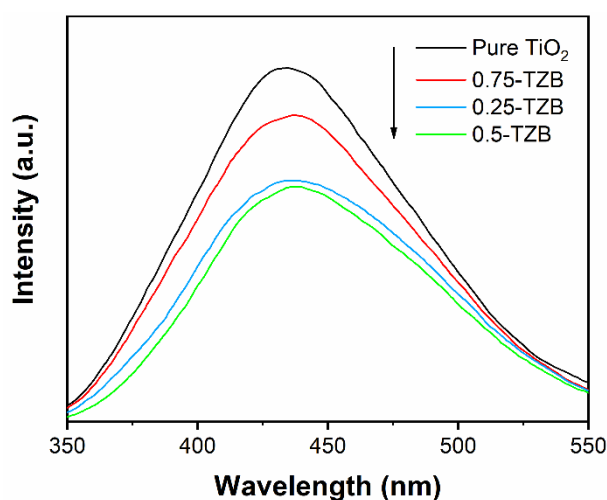


Fig. 4. PL spectra of the different synthesized nanoparticles.

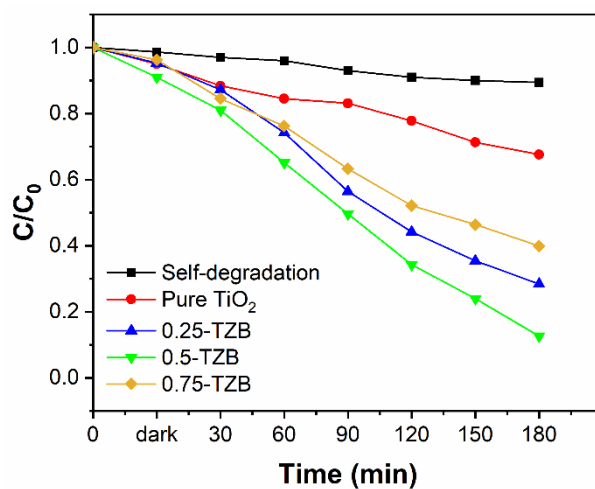


Fig. 5. Photocatalytic degradation of MB using the different TBZ nanoparticles.

visible light illumination, which reveals without addition of the TZB photocatalyst the degradation of MB solution is negligible.

Fig. 6 describes the effect of different amount of the photocatalyst on the degradation efficiency of MB solution was studied using different amount of 0.5-TZB nanoparticles (0.02, 0.04, and 0.06 g). As shown, the optimal amount of the photocatalyst for achieving the highest degradation efficiency is 0.04 g. Further amount leads to dramatic decline in the photocatalytic degradation of MB solution.

This observation can be explained by the fact that the penetration of the light beam is restricted within the turbid dye solution, so the TZB nanoparticles have not access to sufficient light to produce the oxidative radicals [33, 34].

The photocatalytic degradation of MB solution was investigated in the presence of the different concentration of H_2O_2 (0.2, 0.4, and 0.6, mM) as the oxidant agent. Fig. 7 shows the enhancement of the photocatalytic degradation of MB solution upon addition of H_2O_2 over the 0.5-TZB

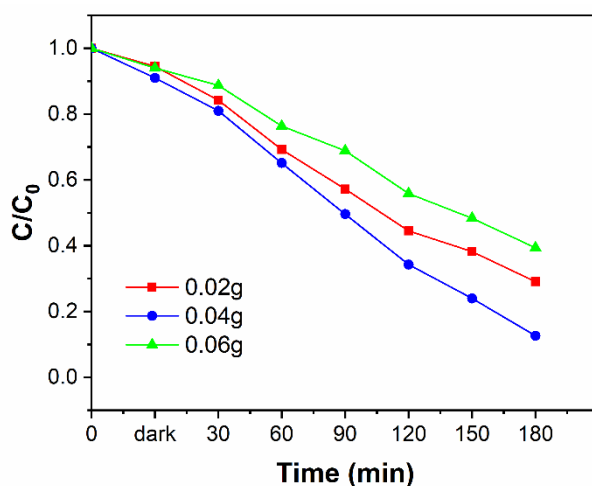


Fig. 6. Effect of different used of 0.5-TZB nanoparticles on degradation level of MB.

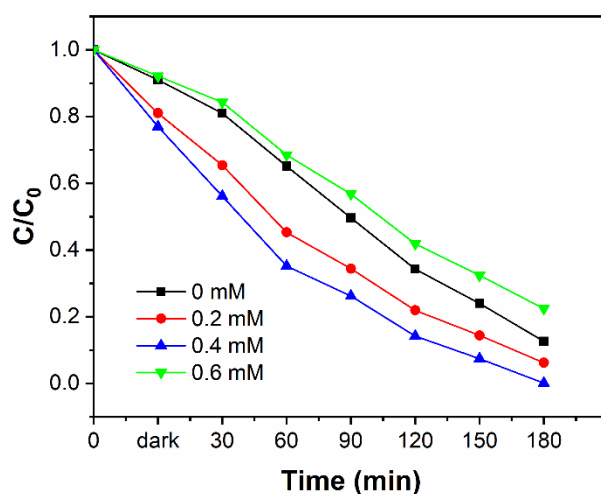


Fig. 7. Photocatalytic degradation of MB using 0.5-TZB nanoparticles in presence of different concentration of H_2O_2 .

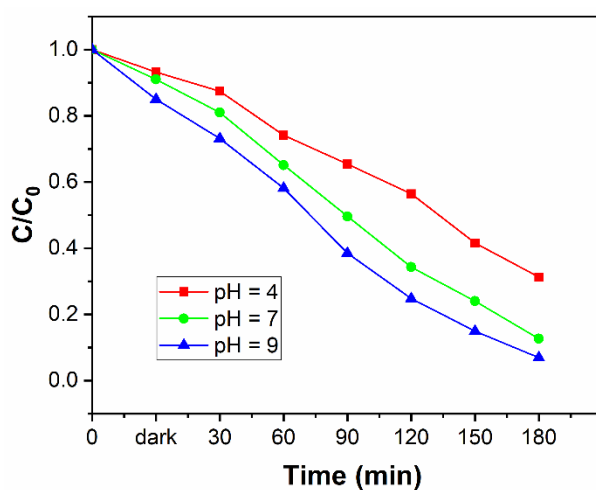


Fig. 8. Photocatalytic degradation of MB using 0.5-TZB nanoparticles under different pH conditions.

photocatalyst. The photocatalytic degradation increased by addition of H_2O_2 up to 0.4 mM, which is attributed to the release of more oxidative radicals for degradation of MB molecules. However, deactivation of radicals is caused by further amount of H_2O_2 giving rise to the decrease of the degradation level [35, 36].

Another important determinant on the photocatalytic performance is the pH of the dye solution. Due to the fact that the photocatalytic reaction takes place on the surface of the photocatalyst, the increased adsorbed dye molecules on the surface of the photocatalyst results to the increase of the degradation level [37]. Therefore, when the photocatalyst surface has opposite charge with respect to the dye molecules, the enhanced adsorption of the dye molecules leads to the increase in the photocatalytic efficiency. On the other hand, there is a repulsion force between the dye molecules and photocatalyst surface with the same charge, pushing the dye molecules away of the active sites on the photocatalyst, and in turn leads to decrement of the photoactivity [38, 39]. Fig. 8 shows the elevation of degradation level in alkaline MB solution. In alkaline condition, the negatively charged surface of the photocatalyst favors the adsorption of a cationic dye like MB [38, 40]. However, there is a significant reduction in photocatalytic degradation under acidic condition.

CONCLUSION

We have demonstrated the $\text{TiO}_2/\text{ZnO}/\text{Bi}_2\text{O}_3$ ternary mixed metal oxide nanoparticles using the simple sol-gel method. The nanoparticles showed the great potential as the visible light photocatalyst confirming by the DRS and PL analysis. An aqueous solution of MB was used to evaluate the photoactivity of the synthesized nanoparticles. The photocatalytic degradation of MB solution approached to more than 87% after 180 min illumination under visible light. To find optimum condition for achieving the highest degradation level of MB solution, various parameters including pH of the dye solution, effect of H_2O_2 , and addition of different amount of the synthesized nanoparticles were carefully investigated.

CONFLICT OF INTEREST

The authors declare that there is no conflict of interests regarding the publication of this manuscript.

REFERENCES

1. Zhu Y-k, Wu L-g, Chen H, Guo H-C, Zheng R, Wang T. The Photocatalytic Degradation Mechanism for Organic Pollutants in Seawater and the Fabrication of Catalyst-Loaded Floating Spheres for Effectively Removing Tetracycline. *The Journal of Physical Chemistry C*. 2024;128(6):2493-2505.
2. Wang F, Xia S, Qin X. Construction and properties of highly

- efficient $\text{Ag}_3\text{Si}_2\text{O}_7/\text{C-WO}_3$ visible light photocatalyst for water purification. *Colloids Surf Physicochem Eng Aspects*. 2025;705:135700.
3. Dai Y, Liu G, Sun X, Ma J, Xian T, Yang H. Mn doping and ZnS nanoparticles modification on Bi_2MoO_6 to achieve an highly-efficient photocatalyst for TC degradation. *Appl Surf Sci*. 2025;681:161611.
4. Zhou Y, Elchalakani M, Du P, Sun C. Cleaning up oil pollution in the ocean with photocatalytic concrete marine structures. *Journal of Cleaner Production*. 2021;329:129636.
5. Daghrir R, Drogui P, Robert D. Modified TiO_2 For Environmental Photocatalytic Applications: A Review. *Industrial and Engineering Chemistry Research*. 2013;52(10):3581-3599.
6. Zeng Q, An W, Peng D, Liu Q, Zhang X, Ge H, et al. Research Progress in Photocatalytic-Coupled Microbial Electrochemical Technology in Wastewater Treatment. *Catalysts*. 2025;15(1):81.
7. Schneider J, Matsuoka M, Takeuchi M, Zhang J, Horiuchi Y, Anpo M, et al. Understanding TiO_2 Photocatalysis: Mechanisms and Materials. *Chem Rev*. 2014;114(19):9919-9986.
8. Armaković SJ, Savanović MM, Armaković S. Titanium Dioxide as the Most Used Photocatalyst for Water Purification: An Overview. *Catalysts*. 2022;13(1):26.
9. Castellote M, Bengtsson N. Principles of TiO_2 Photocatalysis. Applications of Titanium Dioxide Photocatalysis to Construction Materials: Springer Netherlands; 2011. p. 5-10.
10. Wold A. Photocatalytic properties of titanium dioxide (TiO_2). *Chem Mater*. 1993;5(3):280-283.
11. Chakravorty A, Roy S. A review of photocatalysis, basic principles, processes, and materials. *Sustainable Chemistry for the Environment*. 2024;8:100155.
12. Pelaez M, Nolan NT, Pillai SC, Seery MK, Falaras P, Kontos AG, et al. A review on the visible light active titanium dioxide photocatalysts for environmental applications. *Applied Catalysis B: Environmental*. 2012;125:331-349.
13. Guo Q, Zhou C, Ma Z, Yang X. Fundamentals of TiO_2 Photocatalysis: Concepts, Mechanisms, and Challenges. *Adv Mater*. 2019;31(50).
14. Liu L, Chen M, Hu N, Jiang Y, Zeng S, An Y. Precise control of photogenerated carrier behavior of zinc oxide through band reconstruction to enhance photocatalytic treatment of dye wastewater. *Journal of Colloid and Interface Science*. 2025;678:494-505.
15. Abed SH, Shamkhi AF, Heydaryan K, Mohammadalizadeh M, Sajadi SM. Sol-gel Pechini preparation of $\text{CuEr}_2\text{TiO}_6$ nanoparticles as highly efficient photocatalyst for visible light degradation of acid red 88. *Ceram Int*. 2024;50(13):24096-24102.
16. Qian R, Zong H, Schneider J, Zhou G, Zhao T, Li Y, et al. Charge carrier trapping, recombination and transfer during TiO_2 photocatalysis: An overview. *Catal Today*. 2019;335:78-90.
17. Lettieri S, Pavone M, Fioravanti A, Santamaria Amato L, Maddalena P. Charge Carrier Processes and Optical Properties in TiO_2 and TiO_2 -Based Heterojunction Photocatalysts: A Review. *Materials (Basel, Switzerland)*. 2021;14(7):1645.
18. Tuama AN, Alzubaidi LH, Jameel MH, Abass KH, bin Mayzan MZH, Salman ZN. Impact of electron-hole recombination mechanism on the photocatalytic performance of ZnO in water treatment: A review. *J Sol-Gel Sci Technol*. 2024;110(3):792-806.
19. Ahmad I, Zou Y, Yan J, Liu Y, Shukrullah S, Naz MY, et al. Semiconductor photocatalysts: A critical review highlighting the various strategies to boost the photocatalytic performances for diverse applications. *Advances in Colloid and Interface Science*. 2023;311:102830.
20. Shirazi P, Rahbar M, Behpour M, Ashrafi M. $\text{La}_2\text{MnTiO}_6$ double perovskite nanostructures as highly efficient visible light photocatalysts. *New J Chem*. 2020;44(1):231-238.
21. Perumal V, Uthrakumar R, Chinnathambi M, Immozi C, Robert R, Rajasaravanan ME, et al. Electron-hole recombination effect of SnO_2 – CuO nanocomposite for improving methylene blue photocatalytic activity in wastewater treatment under visible light. *Journal of King Saud University - Science*. 2023;35(1):102388.
22. Karthikeyan C, Arunachalam P, Ramachandran K, Al-Mayouf AM, Karuppuchamy S. Recent advances in semiconductor metal oxides with enhanced methods for solar photocatalytic applications. *J Alloys Compd*. 2020;828:154281.
23. Roy SD, Das KC, Dhar SS. Facile synthesis of $\text{CuO-Ag}_2\text{O}$ hybrid metal oxide composite using carica papaya, cooconing with hydroxyapatite, and photocatalytic degradation of organic dyes. *Materials Science and Engineering: B*. 2024;303:117331.
24. Dey A, Gogate PR, Gote YM. A review on ultrasound assisted synthesis of metal oxide and doped metal oxide nanocatalysts and subsequent application as photocatalyst for dye degradation. *Environ Qual Manage*. 2023;33(4):139-163.
25. Zhang H, Chen G, Bahnemann DW. Photoelectrocatalytic materials for environmental applications. *J Mater Chem*. 2009;19(29):5089.
26. Hernández-Alonso MD, Fresno F, Suárez S, Coronado JM. Development of alternative photocatalysts to TiO_2 : Challenges and opportunities. *Energy and Environmental Science*. 2009;2(12):1231.
27. Robert D. Photosensitization of TiO_2 by MxOy and MxSy nanoparticles for heterogeneous photocatalysis applications. *Catal Today*. 2007;122(1-2):20-26.
28. Miyauchi M, Nakajima A, Watanabe T, Hashimoto K. Photoinduced Hydrophilic Conversion of TiO_2/WO_3 Layered Thin Films. *Chem Mater*. 2002;14(11):4714-4720.
29. Li F, Liu G, Liu M, Liu X, Dong L, Wang D, et al. Oxygen vacancies enriched Z-scheme $\text{BiOI}/\text{Bi}_2\text{O}_3$ heterojunction with controllable band-gap for dye degradation and Cr (VI) reduction. *Ceram Int*. 2025;51(7):8647-8657.
30. Abdelaal AM, Morshedy AS, El-Sherif AA, Ahmed YM, Mohamed GG, Mahmoud RMA, et al. Enhanced photocatalytic activity for hydrogen evolution through $\text{NiO}/\text{Bi}_2\text{O}_3$ nanocomposites. *Int J Hydrogen Energy*. 2024;58:1504-1513.
31. Venkatesh G, Palanisamy G, Lee J, Manimaran K, Abu-Yousef I, Kanan S. Synergistic effect of dual Z-scheme $\text{ZnO}/\text{g-C}_3\text{N}_4/\text{V}_2\text{O}_5$ heterogeneous nanocomposite for photocatalytic decontamination of mixed dye and pharmaceutical drug under visible light irradiation. *J Alloys Compd*. 2025;1010:178186.
32. Naeinian N, Imani M, Tadjarodi A. Mechanochemical synthesis of $\text{CoFe}_2\text{O}_4/\text{Bi}_2\text{MoO}_6$ mixed metal oxide and study of its photocatalytic behavior. *Mater Lett*. 2024;355:135512.
33. Anandan S, Sathish Kumar P, Pugazhenthiran N, Madhavan J, Maruthamuthu P. Effect of loaded silver nanoparticles

- on TiO_2 for photocatalytic degradation of Acid Red 88. *Sol Energy Mater Sol Cells*. 2008;92(8):929-937.
34. Sathish Kumar PS, Sivakumar R, Anandan S, Madhavan J, Maruthamuthu P, Ashokkumar M. Photocatalytic degradation of Acid Red 88 using Au- TiO_2 nanoparticles in aqueous solutions. *Water Res*. 2008;42(19):4878-4884.
 35. Rahbar M, Mehrzad M, Behpour M, Mohammadi-Aghdam S, Ashrafi M. S, N co-doped carbon quantum dots/ TiO_2 nanocomposite as highly efficient visible light photocatalyst. *Nanotechnology*. 2019;30(50):505702.
 36. Daneshvar N, Salari D, Khataee AR. Photocatalytic degradation of azo dye acid red 14 in water on ZnO as an alternative catalyst to TiO_2 . *J Photochem Photobiol A: Chem*. 2004;162(2-3):317-322.
 37. Rahbar M, Behpour M. Multi-walled carbon nanotubes/ TiO_2 thin layer for photocatalytic degradation of organic pollutant under visible light irradiation. *Journal of Materials Science: Materials in Electronics*. 2016;27(8):8348-8355.
 38. Azeez F, Al-Hetlani E, Arafa M, Abdelmonem Y, Nazeer AA, Amin MO, et al. The effect of surface charge on photocatalytic degradation of methylene blue dye using chargeable titania nanoparticles. *Sci Rep*. 2018;8(1):7104-7104.
 39. Kazeminezhad I, Sadollahkhani A. Influence of pH on the photocatalytic activity of ZnO nanoparticles. *Journal of Materials Science: Materials in Electronics*. 2016;27(5):4206-4215.
 40. Verma S, Tirumala Rao B, Singh R, Kaul R. Photocatalytic degradation kinetics of cationic and anionic dyes using Au-ZnO nanorods: Role of pH for selective and simultaneous degradation of binary dye mixtures. *Ceram Int*. 2021;47(24):34751-34764.